# Effective Resolution of an Adaptive Rate ADC

Saeed Mian Qaisar, Laurent Fesquet, Marc Renaudin

# Effective Resolution of an *Adaptive Rate ADC*

Saeed Mian Qaisar[(1)], Laurent Fesquet[(1)] and Marc Renaudin[(2)]

(1) TIMA, 46 avenue Félix Viallet, 38031 GRENOBLE Cedex, France.
(2) Tiempo SAS, 110 Rue Blaise Pascal, Bat Viseo – Inovallee, 38330, Montbonnot St Martin, France.
(saeed.mian-qaisar, Laurent.fesquet)@imag.fr, marc.renaudin@tiempo-ic.com

## Abstract:

Most real life signals are of non-stationary nature. An efficient acquisition of such signals can be achieved by adapting the acquisition rate according to the input signal local characteristics. In this context, an ARADC (Adaptive Rate Analog to Digital Converter), based on the level crossing sampling is proposed. The ADC effective resolution is a classical parameter to characterize its performance. In this context, a novel method is devised to measure the ARADC resolution. A criterion for properly choosing the different system parameters in the aim of acquiring the desired effective resolution is also described.

## 1. Introduction

The signal acquisition process dictates the performance of the complete signal processing chain. A smarter signal acquisition results into an efficient system and vice versa [1]. The classical ADCs are time-invariant, hence are parameterized by taking into account the worst possible case for the considered application. They capture the input signal at a constant rate. It causes an increased number of samples to be processed, especially in the case of low activity sporadic signals [2-4, 7-9].

This shortcoming is resolved up to a certain extent by employing the ARADC in various applications [7-9]. The motivation behind the ARADC is to achieve a smart A/D conversion. The idea is to acquire only the relevant signal parts and to adapt the sampling rate according to the input signal local variations. An efficient solution is proposed by smartly combining the features of both the uniform and the non-uniform signal processing tools.

## 2. The ARADC

The block diagram of the ARADC is shown in Figure 1.

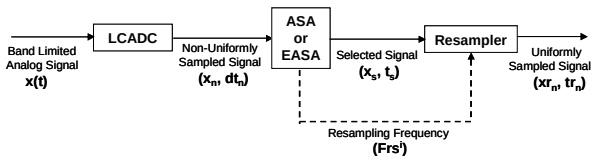


Figure 1: The block diagram of the ARADC.

In the ARADC, a band-limited input signal is acquired by a LCADC (Level Crossing based ADC) [3, 4]. According to [2], the sampling instants of a non-uniformly sampled signal obtained with the LCADC are defined by Equation 1. Where $t_n$ is the current sampling instant, $t_{n-1}$ is the previous one and $dt_n$ is the time delay between the current and the previous sampling instants.

$$t_n = t_{n-1} + dt_n \qquad \text{Eq. 1}$$

LCADCs drastically reduce the activity of the post processing chain, because they only capture the relevant information [3, 4, 7-9]. Let $\Delta V_{in}$ and $\Delta x(t)$ be the LCADC and the input signal $x(t)$ amplitude dynamics respectively. In order to avail the complete LCADC resolution in the studied case, $\Delta x(t)$ is always adapted to match $\Delta V_{in}$. For a $M$-bit LCADC, the maximum and the minimum sampling frequencies are defined by Equations 2 and 3 respectively [7]. Where, $Fs_{max}$ and $Fs_{min}$ are the maximum and the minimum sampling frequencies. $f_{max}$ is the highest and $f_{min}$ is the lowest frequency of $x(t)$.

$$Fs_{\max} = 2.f_{\max}.\left(2^M - 1\right) \qquad \text{Eq. 2}$$

$$Fs_{\min} = 2.f_{\min}.\left(2^M - 1\right) \qquad \text{Eq. 3}$$

LCADCs deliver a non-uniform time repartitioned output. The non-uniformly sampled signal obtained with LCADCs can be used for further non-uniform digital processing [7]. However in the studied case, the non-uniformity of the sampling process, which yields information on the signal local features, is employed to select only the relevant signal parts. Furthermore, the characteristics of each signal selected part are analyzed and are employed later on to adapt the system parameters accordingly. This selection and local-features extraction process is performed by the ASA (Activity Selection Algorithm) or the EASA (Enhanced Activity Selection Algorithm). They split the signal into a series of active windows. A detailed description of these algorithms is given in [8, 9]. The ASA and the EASA display interesting features with the LCSS, which are not available in the classical case. They select only the active parts of the non-uniformly sampled signal, obtained with the LCADC. Moreover, they correlate the length of the selected window with the signal local characteristics. In addition, they provide an efficient reduction of the spectral leakage phenomenon [8, 9].

Finally, the selected signal obtained with the activity selection algorithm is resampled uniformly. The resampling frequency $Frs^i$ of the $i^{th}$ selected window $W^i$ can be specific. According to [8, 9], $Frs^i$ can be computed by employing the following Equations.

$$L^i = t\max^i - t\min^i \qquad \text{Eq. 4}$$

$$Frs^i = \frac{N^i}{L^i} \qquad \text{Eq. 5}$$

Where, $tmax^i$ and $tmin^i$ are the final and the initial times of $W^i$. $L^i$ is the length in seconds and $N^i$ is the number of samples laying in $W^i$. The upper and the lower bounds on $Frs^i$ are $Fs_{max}$ and $Fs_{min}$ respectively.

## 3. The ARADC Resolution

Each stage has its impact on the overall effective resolution. In order to quantify the impact of each stage, the error sources of each stage are discussed and a method to compute the *SNR* (Signal to Noise Ratio) at each step is devised in the following subsections.

### 3.1 The LCADC SNR

Classically during an ideal A/D conversion process, the sampling instants are exactly known, where as samples amplitudes are quantized at the ADC resolution [10, 11], which is defined by the ADC number of bits. This error is characterized by the *SNR*, which can be expressed by Equation 6.

$$SNR(dB) = 6.02 . M + 1.76 \qquad \text{Eq. 6}$$

Here, *M* is the ADC number of bits. It follows that the *SNR* of an ideal ADC depends only upon *M* and it can be improved by 6.02 dB for each increment in *M*.

The A/D conversion process, which occurs in LCADCs, is dual in nature. Ideally in this case, samples amplitudes are exactly known, while the sampling instants are quantized at the timer resolution $T_{timer}$. According to [3, 4], the *SNR* in this case is given by Equation 7.

$$SNR(dB) = -11.19 - 20\log\left(f_{sig}.T_{timer}\right) \qquad \text{Eq. 7}$$

Here, $f_{sig}$ is the input signal frequency. It shows that in this case, the *SNR* does not depend on *M* any more, but on *x(t)* characteristics and $T_{timer}$. An improvement of 6.02 dB in the *SNR* can be achieved by simply halving $T_{timer}$.

Equations 6 and 7 respectively give the theoretical *SNR* of the classical and the level crossing converters. Practically, the A/D converters introduce further errors like the time jitter, the comparator ambiguity, etc in addition to the quantization phenomenon [11]. Usually, the converter practical $SNR_{real}$ is measured from the spectrum of a windowed sequence of the ADC output samples. A method of calculating the converter practical *SNR* is detailed in [12]. By knowing the $SNR_{real}$ of an ADC, its ENOB (Effective Number of Bits) can be calculated by employing the following Equation [10, 11].

$$ENOB = \frac{SNR_{real}(dB) - 1.76}{6.02} \qquad \text{Eq. 8}$$

Theoretically, the LCADC *SNR* can be improved as far as it is required by reducing $T_{timer}$. But practically there is a limit, which is imposed by the analog blocks accuracy [3, 4]. In fact, the analog blocks determine the threshold levels precision. If these levels are known with uncertainty $\Delta a$, then this error must be taken into account and it will result into *SNR* degradation. Usually, the ADC $SNR_{real}$ is computed by employing the spectral analysis [12]. The LCADC output is non-uniformly distributed in time. Hence, its spectrum can not be properly computed with the classical tools. Several methods have been developed for the spectral analysis of the non-uniformly sampled. In [8], performances of the GDFT (General Discrete Fourier Transform) and the Lomb's algorithm are studied for the case of level crossing sampled signal. It is shown that these methods are erroneous because of the presence of wideband spectral noise. Hence, they can not provide a proper calculation of the LCADC $SNR_{real}$.

In context of the above discussion, a novel approach is proposed for the LCADC $SNR_{real}$ measurement. It does not require frequency domain transformation and calculates the *SNR* directly in time domain. The practical ADC is characterized by employing a monotone sinusoid [10, 11]. Therefore a similar signal given by Equation 9 is employed in this case.

$$x(t) = A.\sin\left(2.\pi.f_{sig}.t + \theta\right) \qquad \text{Eq. 9}$$

Here, *A*, $f_{sig}$ and $\varphi$ are the amplitude, the frequency and the initial phase. For the ease of process understanding $\Theta = 0$ is considered in the studied case. In the case of a mono harmonic signal it is possible to analytically calculate the level crossing instants [6]. Thus, in this case $t_n$ can be calculated by employing Equation 10.

$$t_n = \frac{1}{2.\pi.f_{sig}}.\arcsin\left(\frac{level_m}{A}\right) \qquad \text{Eq. 10}$$

Here, $level_m$ is the $m^{th}$ level crossing threshold. Amplitude of the $n^{th}$ level crossing sample $x_n$ can be calculated as: $x_n = level_m$. Hence, by employing this method, firstly an ideal LCSS is implemented for *x(t)*, which provides an exact knowledge of both time-amplitude values of the level crossing samples.

The only error occurs in the ideal LCADC is the time quantization [3, 4]. By assuming that the time error $\delta t$ is uncorrelated to the input signal, it is modeled as a white noise. If $\delta t_n$ is the time quantization occurs for $t_n$, then it can randomly takes a value between *0* and $T_{timer}$. Thus, $tq_n$ (the quantized version of $t_n$) can be obtained by employing Equation 11. The time quantization also affects the amplitude value of the corresponding level crossing sample. The erroneous sample amplitude value is calculated by using Equation 12.

$$tq_n = t_n + \delta t_n \qquad \text{Eq.11}$$

$$xq_n = A.\sin\left(2.\pi.f_{sig}.tq_n\right) \qquad \text{Eq.12}$$

Now the ideal LCADC conversion error per sample point $Cq_n$ is given by the absolute difference between $x_n$ and $xq_n$. The RMS (root mean square) value of *Cq* for *N* level crossing samples can be calculated by employing Equation 13. Finally the *SNR* of an ideal LCADC can be calculated by employing Equation 14.

$$RMS(cq) = \sqrt{\frac{1}{N}.\sum_{n=1}^{N} Cq_n^2} \qquad \text{Eq.13}$$

$$SNR(dB) = \frac{RMS(Signal)}{RMS(Cq)} \qquad \text{Eq.14}$$

In the case of a real LCADC, there also exists error due to the threshold levels ambiguity [3, 4]. Let $\Delta a_n$ is the error introduced due to the quantization levels ambiguity into $xq_n$. Then, the $n^{th}$ erroneous level crossing sample amplitude $xe_n$, contains effect of both $\delta t_n$ and $\Delta a_n$ and it can be calculated by employing Equation 15. The real

LCADC conversion error per sample point $Ce_n$ is given by the absolute difference between $x_n$ and $xe_n$. The RMS (*Ce*) for *N* level crossing samples can be calculated by employing a similar relation, shown by Equation 13. Finally, the LCADC $SNR_{real}$ can be computed as a ratio between the RMS (signal) and the RMS (Ce).

$$xe_n = xq_n \pm \Delta a_n \qquad \text{Eq. 15}$$

### 3.2 The Activity Selection SNR

For a monotone sinusoid, the activity selection algorithm (ASA/EASA) parameters can be easily adjusted to avoid the signal truncation. In this case, the windowing is performed with the adaptive length rectangular function [9]. Since, the employed window shape is rectangular, it has no impact on the ARADC output resolution. It just selects the relevant parts of the LCADC output and passes them to the resampler block (cf. Figure 1).

### 3.3 The Resampler SNR

The resampling process requires interpolation, which changes properties of the resampled signal compared to the original one [5]. For the practical LCADC, there exist uncertainties in the time-amplitude pairs of the level-crossing samples (cf. Section 3.1). These uncertainties accumulate in the interpolation process and deliver the overall error at the ARADC output.

If ($tr_n$, $xr_n$) represents the time-amplitude pair of the $n^{th}$ interpolated sample. Then the $n^{th}$ reference sample amplitude $xo_n$, which should be obtained by sampling $x(t)$ at $tr_n$, can be calculated by employing the following Equation.

$$xo_n = A.\sin\left(2.\pi.f_{sig}.tr_n\right) \qquad \text{Eq. 16}$$

The resampling error per interpolated observation $Ie_n$ is given by the absolute difference between $xo_n$ and $xr_n$. The RMS (*Ie*) for *N* resampled observations can be calculated by employing a similar relation to Equation 13. Finally, the ARADC $SNR_{real}$ can be computed as a ration between the RMS (signal) and the RMS (*Ie*).

## 4. The Simulation Results

In order to illustrate the proposed method, a simulation is performed. In this case, $x(t)=V_{max}.sin(2.\pi.2300.t)$ is employed as input. $V_{max} = 0.9$ v is chosen.

Equation 7 shows that for a fixed $f_{sig}$, the ideal LCADC *SNR* varies as a function of $T_{timer}$. In order to demonstrate this statement, the simulations are performed for fixed $M=3$ and by varying $T_{timer}$ between $[2^0; 2^{-2}]$ µs. The ideal LCADC *SNR* is measured by employing Equation 14. The obtained results are summarized in Table 1.

| $T_{timer}$ (µs) | $SNR_{LCADC-TH}$ (dB) | SNR (dB) |
|---|---|---|
| $2^0$ | 41.58 | 41.21 |
| $2^{-1}$ | 47.60 | 47.44 |
| $2^{-2}$ | 53.62 | 53.44 |

Table 1: The ideal LCADC SNR for fixed $M$=3 and varying $T_{timer}$.

In Table 1, $SNR_{LCADC-Th}$, represents the LCADC theoretical SNR, computed for the given parameters by employing Equation 7. These results show accordance between $SNR_{LCADC-Th}$ and the obtained *SNR*, which verifies the authenticity of the proposed LCADC *SNR* measurement method.

Although the LCADC *SNR* is independent of *M*, yet an appropriate value of *M* should be chosen in order to ensure a proper reconstruction of the acquired signal [3, 4, 7-9].

In the case of a practical LCADC, the threshold levels ambiguity error $\Delta a$ also occurs along with the time quantization error $\delta t$. The modeling of $\Delta a$ is not straight forward and it depends upon the circuit architecture and technology employed for its implementation. A study on $\Delta a$ for different LCADC implementations is out of the scope of this article. Here, the example of the AADC [4], is taken into account. In this case, the threshold levels are generated with the DAC (D/A Converter). Hence, a 3-bits DAC is implemented in the Cadence circuit design tool using the STMicroelectronics 0.13-µm CMOS technology.

$\Delta a$ mainly occurs because of the process and the mismatch variations, introduced during the circuit fabrication. The effect of the process and the mismatch variations on $v_{out}$ (threshold level) is studied for different input combinations by employing Monte Carlo simulations. It is found that due to the effect of process variations $v_{out}$ varies within the range of $\pm 0.21\%$ *of* $v_{out}$. Similarly, due to the mismatch variations $v_{out}$ varies within the range of $\pm 0.11\%$ *of* $v_{out}$. Finally, the variation of $v_{out}$ due to the combined effect of process and mismatch variations is calculated and it is $\pm 0.23\%$ *of* $v_{out}$. Following this, $\Delta a$ is chosen equal to $\pm 0.23\%$ *of* $x_n$ and $xe_n$ is computed by employing Equation 15. The practical LCADC $SNR_{real}$ is computed by employing the method discussed in Section 3.1.

The simulation is performed for the same parameters, employed in the case of ideal LCADC. The obtained results are summarized in Table 2.

| $T_{timer}$ (µs) | $SNR_{LCADC-TH}$ (dB) | $SNR_{real}$ (dB) | ENOB (dB) |
|---|---|---|---|
| $2^0$ | 41.58 | 41.16 | 6.54 |
| $2^{-1}$ | 47.60 | 47.05 | 7.52 |
| $2^{-2}$ | 53.62 | 52.88 | 8.49 |
| $2^{-3}$ | 59.64 | 56.71 | 9.13 |
| $2^{-4}$ | 65.66 | 58.93 | 9.50 |
| $2^{-5}$ | 71.66 | 59.45 | 9.58 |

Table 2: The real LCADC SNR for fixed $M$=3 and varying $T_{timer}$.

Here, *ENOB* values are calculated by employing Equation 8. In a practical LCADC, the conversion error mainly consists of $\delta t$ and $\Delta a$. Table 2 demonstrates that how $\Delta a$ is limiting the *ENOB*. In the studied case, for higher $T_{timer}$ values $[2^0; 2^{-2}]$ µs, the major error occurs because of $\delta t$ and the employed value of $\Delta a$ has minor impact on the $SNR_{real}$. Contrary, with a further reduction of $T_{timer}$ the error occurs because of $\Delta a$ is getting significant compared to the error introduced by $\delta t$. Hence, for lower $T_{timer}$, $\Delta a$ is the main limiting factor on the $SNR_{real}$ improvement. For the employed $\Delta a$, the limit on the achievable $SNR_{real}$ is around 59 dB for $T_{timer}=2^{-5}$ µs. Further reduction in $T_{timer}$ will not introduce

noteworthy gain in the $SNR_{real}$, except by achieving an appropriate reduction in $\Delta a$.

The selected signal obtained at the ASA/EASA output is resampled uniformly (cf. Figure 1). A large range of interpolation functions is available. Computationally efficient solutions, such as the NNR (Nearest Neighbor Resampling) and the linear interpolations are employed for the resampling purpose.

For a fixed $T_{timer}$, the resampled data *SNR* increases with the increase in *M*. The reason behind is that for any kind of employed interpolation, the upper bound on $Ie_n$ is imposed by *q* [8]. Here, *q* is the LCADC quantum and is given as: $q=2V_{max}/(2^M-1)$. Here, $V_{max}$ is the LCADC half amplitude range. It follows that an increase in *M* causes a reduction in *q*, which consequently results into a reduced $Ie_n$.

The *SNR* of the uniformly sampled data, obtained in cases of the NNR and the linear interpolations is calculated by employing the method discussed in Section 3.3. It is performed by varying *M* and $T_{timer}$ between [3; 8] and $[2^2; 2^{-5}]$ μ seconds respectively.

The ARADC conversion error mainly consists of $\delta t$, $\Delta a$ and *Ie*. Once the threshold levels are established, $\Delta a$ remains constant [3]. For given $\Delta a$ once $T_{timer}$ is decided, then the next step is an appropriate choice of *M* and the interpolation order. From simulation results it is found that while employing the linear interpolation, $M=8$ is sufficient to approach the upper $SNR_{real}$ bound of 59 dB. On the other hand, in the NNR interpolation case, $M=10$ bits is required to achieve the upper $SNR_{real}$ bound. It follows that for certain $\delta t$ and $\Delta a$, the upper achievable $SNR_{real}$ bound can be obtained for lower *M* with the increase in interpolation order. As an example, the same $SNR_{real}$ bound can be achieved for $M=4$ and $T_{timer}=2^{-5}$ μ seconds, while performing the resampling with a fourth order interpolator. Note that higher order interpolators provide better results at the cost of an increased computation per resampled observation. Therefore, an appropriate interpolation order should be employed, which keeps the system computationally efficient, while not much affects the $SNR_{real}$ for the chosen parameters.

In order to compare the ARADC performance with the classical ADC, their SNR curves are plotted on Figure 2. The SNR values for the classical case are obtained by employing Equation 6.

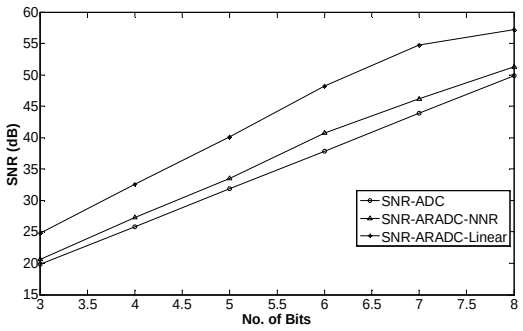


Figure 2: The SNR curves for the ADC and the ARADC.

In Figure 2, $SNR_{ARADC\text{-}NNR}$ and the $SNR_{ARADC\text{-}Linear}$, represent $SNR_{ARADC}$ obtained in the case of the NNR and the linear interpolations respectively. Figure 2 shows that in the studied case, for each value of *M* the $SNR_{ARADC\text{-}NNR}$ and the $SNR_{ARADC\text{-}Linear}$ remain higher than the corresponding classical one. It shows that for an appropriate choice of $T_{timer}$, $\Delta a$ and the interpolation order, a higher ENOB can be achieved for a given *M*, in the case of ARADC compared to the classical ADC.

## 5. Conclusion

The ARADC is well suited for low activity sporadic signals. For such signals, it leads towards a drastic computational gain compared to the counter classical approaches [7-9]. A novel method to compute the ARADC SNR has been devised. It is shown that results obtained with the proposed method are in coherence with the theoretical ones, which verifies the proposed approach correctness. The ARADC SNR depends on *M*, $T_{timer}$, $\Delta a$ and the interpolation order. For a targeted application, an appropriate set of these parameters should be found, which provides an attractive trade off between the system computational complexity and the delivered output quality, while ensuring the proper signal reconstruction.

## References:


[1] I. Bilinskis, “Digital alias free signal processing”, John Wiley and Sons, Ltd, 2007.

[2] J.W. Mark and T.D. Todd, “A nonuniform sampling approach to data compression”, IEEE Transactions on Communications, vol. COM-29, pp. 24-32, 1981.

[3] N. Sayiner et al., “A Level-Crossing Sampling Scheme for A/D Conversion”, IEEE Transactions on Circuits and Systems, vol. 43, pp. 335-339, 1996.

[4] E. Allier et al., “A new class of asynchronous A/D converters based on time quantization”, ASYNC’03, pp.197-205, 2003.

[5] S. de Waele et al., “Time domain error measures for resampled irregular data”, IEEE Transactions on Instrumentation and Measurements, pp.751-756, 1999.

[6] M. Gretains, “Time-frequency representation based chirp like signal analysis using multiple level crossings”, EUSIPCO’07, pp.2154-2158, 2007.

[7] S.M. Qaisar et al., “Computationally efficient adaptive rate sampling and filtering”, EUSIPCO’07, pp.2139-2143, 2007.

[8] S.M. Qaisar et al., “Spectral Analysis of a signal Driven Sampling Scheme”, EUSIPCO’06, 2006.

[9] S.M. Qaisar et al., “Computationally efficient adaptive resolution short-time Fourier transform”, EURASIP, RLSP, 2008.

[10] W. Kester, “Data conversion handbook”, Elsevier/Newnes, 2005, ISBN 0-7506-7841-0.

[11] R.H. Walden, “Analog-to-Digital converter survey and analysis”, IEEE journal on selected areas in communications, vol. 17, No. 4, April 1999.

[12] B. C. Baker, “What does the ADC SNR mean”, Microchip Technology Inc., technical note, 2004.